JOURNAL OF GEOPHYSICAL RESEARCH, VOL. 115, D10203, doi:10.1029/2009JD013053, 2010

Assessment of ISCCP cloudiness over the Tibetan Plateau using CloudSat-CALIPSO

Catherine M. Naud[1] and Yong-Hua Chen[1]

Received 21 August 2009; revised 23 December 2009; accepted 30 December 2009; published 18 May 2010.

[1] Cloudiness over the Tibetan Plateau is difficult to estimate because ground-based measurements are sparse. Satellite observations are thus the best tool and one of the longest climatologies available, the International Satellite Cloud Climatology Project (ISCCP), relies on passive remote sensing to characterize cloud cover and altitude. Active remote sensing from space is used to assess the accuracy of the ISCCP observations over the Tibetan Plateau. August 2006 is chosen to conduct the assessment and compared to February 2007. Cloud cover from ISCCP is underestimated by about 18%, in part because of misdetection of low-level clouds at night. ISCCP cloud top pressures are overestimated by about 150–200 mb in August and 60–130 mb in February. However, the most accurate ISCCP cloud top pressures, with a maximum bias of about 50 mb, are obtained when there are thick single-layer clouds. Within the region, there is no evidence that the differences are directly dependent on elevation. Problems identified in other regions, such as multilayer clouds and optically thin clouds, explain most of the discrepancies in our study region. These results indicate that ISCCP cloud retrievals can be used to compile a realistic climatology at the highest altitudes where single-layer clouds dominate and that the retrievals are most accurate in winter.

Citation: Naud, C. M., and Y.-H. Chen (2010), Assessment of ISCCP cloudiness over the Tibetan Plateau using CloudSat-CALIPSO, *J. Geophys. Res.*, *115*, D10203, doi:10.1029/2009JD013053.

1. Introduction

[2] High-altitude regions have been found to experience a greater rate of warming than most regions on Earth [*Beniston et al.*, 1997; *Beniston*, 2003]. The Tibetan Plateau, the highest and largest plateau in the world, has undergone significant changes during the last decades as revealed from different geophysical fields: an overall warming [*Liu and Chen,* 2000; *You et al.*, 2008 and references therein], precipitation and humidity increase in most places [*Niu et al.*, 2004; *You et al.*, 2008; *Rangwala et al.*, 2009], changes in cloud amount [*Niu et al.*, 2004; *Duan and Wu,* 2006], a general retreat in glaciers, especially in the south [*Li et al.*, 1998; *Yao et al.*, 2004] and modifications in land/permafrost properties [*Wu and Zhang*, 2008; *Cui and Graf,* 2009]. The Tibetan Plateau had the highest rate of warming in the northern hemisphere between 1955 and 1996 [*Liu and Chen*, 2000], with an even greater rate when extending the record to 2007 [*Wang et al.*, 2008]. Because this region plays an important role in both the regional climate and the global atmospheric circulation and is a vital source of fresh water for the most populated area on Earth, it is paramount to understand its climate and the causes of its high rate of warming.

[3] Changes in cloudiness can have a warming or a cooling effect in the Tibetan Plateau [*Duan and Wu*, 2006]; therefore it is important to derive a long-term cloud climatology in this remote region. Surface observations in this region are sparse, so satellite observations are the best source of information. The International Satellite Cloud Climatology Project (ISCCP [*Rossow and Schiffer*, 1999]) provides a long-term climatology of global cloudiness and should help in understanding the influence of cloudiness in high-elevation regions. However, there are some known problems with this data set, and although it has been evaluated against a multitude of independent measurements [*Liao et al.*, 1995a, 1995b; *Jin et al.*, 1996; *Stubenrauch et al.*, 1999a, 1999b; *Rossow and Schiffer,* 1999 and references therein], its accuracy over the Tibetan Plateau and other high-altitude regions is still largely unknown. *Li et al.* [2006] recently compared ISCCP seasonal cloud type frequency against surface based observations over the Tibetan Plateau. However, they did not investigate the reasons for discrepancy (e.g., more than 20% underestimate in cloud amount, and an overestimate in middle-level clouds) and whether these were specific to this high-altitude region or similar to other regions.

[4] We assess the accuracy of the ISCCP seasonal cloudiness over the Tibetan Plateau by using measurements from the first cloud radar in space CloudSat [*Stephens et al.*, 2002] and the coincident lidar measurements of CALIOP

[1]Department of Applied Physics and Applied Mathematics and Goddard Institute for Space Studies, Columbia University, New York, New York, USA.

0148-0227/10/2009JD013053

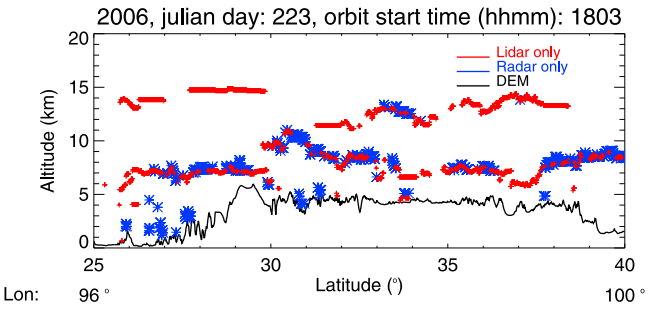

Figure 1. GEOPROF-LIDAR cloud top heights (above mean sea level) of up to 5 cloud layers. Distinguishing heights detected with the lidar (red crosses) from those detected with the radar (blue asterisks). The solid line represents the surface elevation as given in the GEOPROF-LIDAR files. This orbit occurred on 11 August 2006 with a start time of 1803 UTC and intersected the Tibetan Plateau between 40°N–100°E and 25°N–96°N.

onboard CALIPSO [*Winker et al.*, 2009]. These two NASA instruments are part of the A-train and follow the same orbit, with a mere 15 s lag. These active instruments provide a full vertically resolved cloud profile measurement, which allows the identification of complicated situations such as thin cirrus over low-level clouds that can cause problems for passive remote sensing. The radar and lidar have very narrow fields of view, so not all points on Earth can be sampled with these instruments. This can create problems for comparisons with instruments that have a much wider view. We propose a method to adapt these measurements to mimic as best as possible the sampling capability of the ISCCP observations.

[5] We define the Tibetan Plateau region as the area within 25°–40°N and 80°–105°E and select high-resolution (nominal 30 km) 3 hourly ISCCP stage DX products [*Rossow and Schiffer*, 1999] that encompass this area during one summer and one winter month. We conjunctly extract cloud information from the CloudSat-CALIPSO observations obtained over the same region. The first comparison is for the month of August 2006 and assesses the strengths and weaknesses of the ISCCP DX cloud products during a season when a large variety of cloud types should occur. We also perform the same comparison for the month of February 2007, to determine whether any differences we find are dependent on season. We then discuss how problems in the cloud retrievals may impact the ISCCP D1 seasonal cloud climatology over the Tibetan Plateau during the first CloudSat-CALIPSO year (from July 2006 to June 2007).

2. Data and Method

2.1. CloudSat-CALIPSO Cloud Products

[6] In this study, we use cloud information available in the joint CloudSat-CALIPSO product called GEOPROF-LIDAR [*Mace et al.*, 2009]. These files contain the cloud base and cloud top heights of up to 5 layers at the CloudSat horizontal resolution of ~1.1 km (across and along track). A complete description on how the CloudSat and CALIPSO cloud masks are merged to create this joint product is given by *Mace et al.* [2009]. CloudSat can detect most clouds but because of some sensitivity limitations, the radar will miss some cloud layers when they have low water content or small particles. On the contrary, CALIPSO is extremely sensitive to optically thin clouds, but the beam is attenuated when clouds are thick, so information on cloud base and on any lower cloud layer is not available. Thus a synergy between the two measurements can provide a better cloud profile with very little limitations. Consequently, the GEOPROF-LIDAR cloud layers are detected with one or both instruments, as illustrated in Figure 1, that shows an example of a CloudSat-CALIPSO orbit over the Plateau, that occurred near 1800 UTC on 11 August 2006.

[7] Unless otherwise stated, in this study we will use the cloud top height of the highest cloud layer in the joint product, and will refer to it as "CloudSat-CALIPSO," whether it was detected with the lidar or both lidar and radar. We also collect the number of separate cloud layers along each ~1.1 km profile and the cloud top height of the lowest cloud layer when at least 2 layers are present, and refer to it as "first layer."

[8] A lidar is much more sensitive to optically thin clouds or clouds that contain small particles than a radar. Thus sometimes we will test if a given cloud top height was detected by both instruments or only with the lidar by comparing the joint product with the cloud top height obtained with the radar alone. For this, we will use the GEOPROF files [*Marchand et al.*, 2008]. These files contain the cloud mask derived with CloudSat observations, at the same horizontal resolution as the GEOPROF-LIDAR files. The cloud top heights of the highest layer in the GEOPROF cloud mask will be referred to as "CloudSat-only."

[9] Because the ISCCP cloud top information is expressed as a pressure, European Centre for Medium-Range Weather Forecast (ECMWF) reanalysis geopotential height profiles projected onto the CloudSat-CALIPSO orbit are used to convert the CloudSat-CALIPSO and CloudSat-only cloud top heights into pressures. The GEOPROF-LIDAR files also contain the surface altitude for each profile, as obtained from a digital elevation model (DEM), which we also convert into pressures. To summarize, we will use cloud top height and pressure for CloudSat-CALIPSO and CloudSat-only of the highest cloud layer detected in the ~1.1 km horizontal resolution vertical profiles. Other products are extracted: the cloud top pressure of the CloudSat-CALIPSO lowest cloud layer when more than one are present, the total number of cloud layers detected per CloudSat-CALIPSO profile, and the surface height and pressure.

[10] There are some known issues with the two active instruments. For example, the surface return is strong in the radar measurements and contaminates the returns up to 1.2 km above the surface, making it impossible to decipher the hydrometeor from the surface signals [*Marchand et al.*, 2008]. This can cause false cloud detections near the surface. However, we find that less than 0.5% of all the profiles we used in our study contain this ambiguity. Nevertheless, if the highest cloud top in a GEOPROF-LIDAR profile is within 1.2 km of the surface and only detected with the radar, the profile is discarded. We find that this has no effect on the average cloud top pressures, but because this problem is found to occur preferentially in

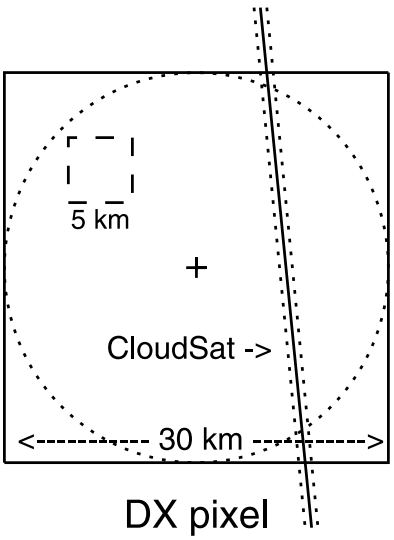

Figure 2. Schematic of a typical intersect between the CloudSat-CALIPSO (CSC) orbit (solid transverse line. The dotted lines on each side indicating ±0.5 km) going through a DX pixel (30 × 30 km square). The cross gives the position of the center of the DX pixel for which a latitude and longitude are given, the dashed square indicates the possible location of the observed 5 × 5 km pixel, and the dotted circle shows the area within 15 km of the DX pixel center.

clear regions, the CloudSat-CALIPSO cloud amount is overestimated if the profiles are retained. We could have considered these profiles to be clear, but because this is not necessarily the case, this could affect our statistics.

[11] The lidar on the other hand suffers from some misidentifications of clouds and aerosols, i.e., some cloud detections may be in fact aerosols, and this also tends to occur near the surface but in regions close to dust or smoke sources [*Liu et al.*, 2009]. Smoke should not be an issue over the Tibetan Plateau, but dust may be in summer [*Tegen and Fung*, 1994], although *Liu et al.* [2009] find that this affects less than 4% of the profiles collected near source regions. Consequently we keep these profiles.

2.2. ISCCP DX Cloud Products

[12] The ISCCP DX observations are available, every 3 h, as 30 × 30 km pixels that contain, among other parameters, the cloud top pressure derived with an infrared channel (IR). A detailed description of the algorithm is given by *Rossow and Schiffer* [1991 and references therein]. During daytime, a correction is applied to the IR cloud top pressures based on information acquired on cloud optical thickness with a visible channel (VIS). The visible channel allows for a correction of cloud top temperatures when the cloud optical thickness is small [*Rossow and Schiffer,* 1991]. So here we use two different DX cloud top pressures, one available all day long because it is solely derived with the IR channel (referred to as "IR") and the other only available during the daytime hours, which is the VIS corrected cloud top pressure (referred to as "VIS"). The DX cloud top pressures (IR and VIS) are in fact derived from a single 4 to 8 km pixel (~5 km on average), but, because of uncertainties in geolocation, this pixel is deemed representative of a larger 30 × 30 km area [*Rossow and Schiffer*, 1991]. This sampling strategy was initially introduced to cope with the large volume of processed data, and tests revealed a good statistical agreement between keeping all ~5 km pixels and sampling pixels every 30 km in a given region [*Sèze and Rossow,* 1991a,1991b; *Rossow,* 1993], only rare and extreme events are affected by the sampling resolution.

2.3. ISCCP D1 Products

[13] For the ISCCP D1 3 hourly data sets, the DX pixels are collected in 280 km equal area grid cells and arranged into a 42 bin histogram that shows the number of cloudy pixels in 7 possible pressure levels and 6 possible optical thickness ranges during the daytime hours. These histograms are summed over all the optical thickness bins and are used to study the seasonal cloud top pressure variations.

2.4. Comparison Method

[14] A given CloudSat-CALIPSO orbit is segmented by selecting profiles that are within 15 km of the center of the 30 × 30 km DX pixel. Figure 2 shows a schematic that represents a possible intersect between a CloudSat-CALIPSO orbit and a DX 30 km pixel. The portion of the CloudSat-CALIPSO orbit selected to match the ISCCP DX pixel is delimited by the 15 km radius circle centered within the 30 × 30 km pixel (the possible location of the 5 km pixel where the ISCCP radiances are observed and processed is also represented in Figure 2). All orbit segments are not 30 km long, they can be shorter if the orbit is close to the 30 km pixel edge. For August 2006 (we obtain virtually identical numbers for February 2007), the average orbit segment is 26 ± 7 km long for 5849 intersects (~23 profiles on average). As mentioned above, the ISCCP DX cloud top pressures are obtained from a 5 × 5 km pixel within a 30 × 30 km region. This means that the area sampled by this smaller pixel is about 25 km^2. A CloudSat transect is about 1 km wide, thus a ~26 km long segment would sample an area equivalent to a DX subpixel. In addition to proximity, a time constraint is applied: the profiles selected along the CloudSat-CALIPSO orbit to construct the DX-like observations have to be obtained within 90 min of the 3 hourly DX observations. There will be obvious limitations as a perfect space and temporal match cannot be achieved, but for overcast situations, and on average over a month, the comparison is possible as variability is limited at resolutions below 30 km [e.g., *Sèze and Rossow,* 1991b].

[15] Within the area observed in a DX pixel (~25 km^2), the visible and IR radiances used for the cloud retrievals represent an average of the signal emitted by both clouds and the surface if the clouds are not overcast. Consequently, the cloud top pressure reported for each DX pixel represents a radiatively weighted average of the cloud top and surface pressures [*Rossow and Schiffer,* 1999]. In order to account for the small-scale (≤~5 km) variations, we averaged cloud top pressures and surface pressures (in cloud-free profiles) along the DX-like CloudSat-CALIPSO orbit segments, and calculated also the standard deviation. This ensures a better comparison in cases when there are broken clouds within the

Table 1. Number of Pixels per Cloudy-Clear Class for the Comparison Between ISCCP DX Pixels and CloudSat-CALIPSO[a]

	CloudSat-CALIPSO DX-like Cloud Fraction		
ISCCP DX	0	1	0 < and < 1 (intermediate)
Clear	293	923	617
Cloudy	72	3594	350

[a]Using the cloud fraction in ~26 km orbit segment for the latter, divided between no cloud (0), overcast (1) and intermediate cloud fraction. ISCCP, International Satellite Cloud Climatology Project.

30×30 km^2 area, when cloud optical properties are highly variable, or when thin semitransparent clouds are present. Each DX-like segment is then considered clear if it contains no or only one cloudy profile. We calculate a cloud fraction as the ratio of the number of CloudSat-CALIPSO cloudy profiles over the total number of profiles found within the DX-like segment. For each segment, we also calculate the average CloudSat-CALIPSO cloud top height (of the highest cloud, also using surface heights for clear profiles), the GEOPROF (CloudSat-only) cloud top pressure (averaged again with surface pressure for the clear profiles), the median number of cloud layers, and the average elevation.

[16] For comparison with the D1 ISCCP products, the same segmentation and cloud top pressure averaging techniques are applied to the CloudSat-CALIPSO products, but this time the segment length is fixed. We use 26 km based on the average segment length found above. Because the 26 km portions do not necessarily match a DX pixel, they are arbitrarily divided. These DX-like cloud top pressures are then organized into histograms for each $2.5° \times 2.5°$ D1 grid cell by counting the number of DX-like cloud top pressures that fall into one of the ISCCP pressure intervals. This is done for each GEOPROF-LIDAR file that intersected a given D1 grid cell. Then all the histograms per grid cell are summed over all the GEOPROF-LIDAR files available per season: spring (MAM), summer (JJA), fall (SON) and winter (DJF). To compare CloudSat-CALIPSO with ISCCP histograms, all grid cell histograms are added together and normalized to the total number of cloud detections. The GEOPROF-LIDAR files intersect the Tibetan Plateau region twice a day near 0600 UTC and 1800 UTC. Because the ISCCP D1 histograms are only available during the daytime hours, only the 0600 UTC D1 files are compared with the CloudSat-CALIPSO histograms obtained around 0600 UTC. For the comparison with DX, both crossing times are kept and only the ISCCP IR cloud top pressures are used for the nighttime crossing.

3. Comparison Between DX ISCCP and CloudSat-CALIPSO Cloud Properties

[17] We start with the high-resolution ISCCP DX products for the month of August 2006. Summer is the monsoon season over the Plateau and includes both synoptic (large) scale and convective (local) scale cloud events. Because of data volume constraints, a month is a good compromise to ensure a reasonable sampling. First we assess cloud detection performance and then compare cloud top pressures. We then conduct the same comparison for a winter month (February 2007) to determine whether our results are season specific.

3.1. Cloud Detection Assessment

[18] First we investigate the agreement between the two cloud masks. For the Tibetan Plateau area and the entire month of August 2006, 5849 pixels were available for comparison. They are distributed between 2543 daytime (43%) and 3306 (57%) nighttime observations.

[19] For CloudSat-CALIPSO, we distinguish the DX-like portions that were totally clear (one profile or none with clouds) and those that were fully covered (all profiles have a cloud top pressure), from those with intermediate cloud fractions (ratio of the number of cloudy profiles to the total number of profiles in the DX-like portion). Table 1 gives the number of pixels for each subset defined by either cloudy or clear ISCCP DX pixel and CloudSat-CALIPSO cloud fraction (0, 1 or intermediate).

[20] If clouds are not overcast in the 30×30 km DX pixel, because ISCCP and DX-like CloudSat-CALIPSO pixels do not necessarily observe the exact same location on Earth, there may be a greater propensity for the two data sets to disagree when the DX-like Cloudsat-CALIPSO cloud fractions are intermediate (strictly between 0 and 1). For the 967 (17%) of the pixels for which CloudSat-CALIPSO cloud fractions are intermediate, ISCCP detects clouds for 350 pixels that have a median CloudSat-CALIPSO cloud fraction of 0.7 and detects none for 617 pixels that have a median CloudSat-CALIPSO cloud fraction of 0.6. As CloudSat-CALIPSO cloud fractions decrease we expect a greater chance for ISCCP to indicate clear sky. However, the similarity in median cloud fraction between the two subsets does not indicate that disagreements between ISCCP and CloudSat-CALIPSO in cloud cover can be attributed to low CloudSat-CALIPSO cloud fractions. However, because these low cloud fractions indicate variability in cloudiness within the 30 km DX pixel, these pixels will not be retained in the rest of our comparison.

[21] When the CloudSat-CALIPSO cloud fraction is 0 or 1, both data sets (i.e., CloudSat-CALIPSO and ISCCP) agree that there are clouds for 3594 pixels (61%) and agree that there are no clouds for 293 pixels (5%). Then, as shown in Table 1, ISCCP indicates clear and the CloudSat-CALIPSO cloud fraction is exactly 1 for 923 pixels (~16%), while ISCCP detects clouds undetected with CloudSat-CALIPSO for only 72 pixels (~1%).

[22] More than two thirds of the 923 pixels occurred at night when the ISCCP visible channel is not available. It is well known that passive remote sensing can be challenging at night [e.g., *Rossow and Garder*, 1993; *Liu et al.*, 2004]. The distribution of cloud top heights above the surface for these 923 pixels shows a large difference for clouds within 4 km of the surface when compared with the same histogram constructed with the 3594 pixels where ISCCP detects clouds (Figure 3). These predominantly nighttime low-level clouds have, on average, vertical extents of 1.6 ± 0.7 km, a top height 2.6 ± 0.8 km above the surface, in areas where the surface is 3.7 ± 1.7 km above mean sea level and where changes in topography are small (0.18 ± 0.17 km standard deviation of surface altitude). The daytime misdetections

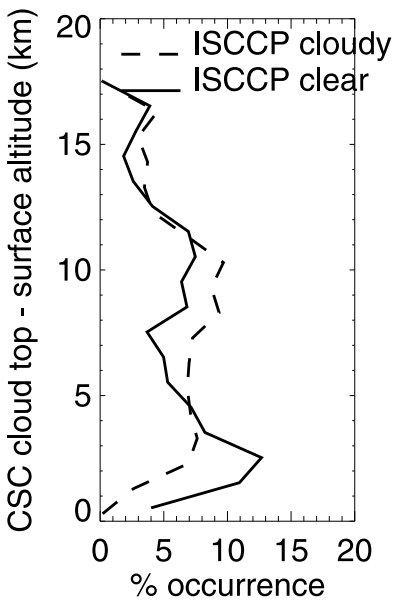

Figure 3. Distribution of CloudSat-CALIPSO (CSC) cloud top heights above surface for all clouds detected by International Satellite Cloud Climatology Project (ISCCP) and CSC (dashed line) and those only detected by CSC (solid line).

affect clouds much closer to the surface than at night (not shown). These misdetections are consistent with previous reports of underestimates of low-level cloud amounts with ISCCP [*Rossow et al.*, 1993; *Jin et al.*, 1996].

[23] The relative difference in average cloud fraction between CloudSat-CALIPSO and ISCCP DX, calculated in the ISCCP 2.5° × 2.5° grid cells covering the Tibetan Plateau (60 cells total) for August 2006, has a mean of 18 ± 11%. This cloud amount underestimate of ISCCP is slightly larger than what previous studies reported [*Rossow and Schiffer*, 1999 and references therein]. This has little to do with our removing profiles with CloudSat-only cloud top heights within 1.2 km of the surface (see discussion at the end of section 2.2). However, CloudSat-CALIPSO should be more sensitive to clouds than the previous instruments used for comparison with ISCCP. In addition, only a month of data is investigated here. These differences tend to increase from northwest to southeast (not shown), and no correlation was found with the average or the standard deviation of the surface altitude per D1 grid box. The ISCCP snow-ice flag indicates no snow nor ice for all the 2.5° resolution grid cells. But using higher-resolution measurements, *Pu and Xu* [2009, Figure 2] show that fractional snow cover is larger to the west than to the east in summer over the plateau, so the presence of snow does not explain the detection issues for this month.

3.2. Cloud Top Pressure Assessment

[24] There are 3594 pixels with both instruments detecting clouds (removing pixels where CloudSat-CALIPSO cloud fraction is less than one), 1826 at night (51%) and 1768 during the day (49%). The average difference between ISCCP IR and VIS and CloudSat-CALIPSO cloud top pressures is summarized in Table 2, and the cloud top pressure distributions are shown in Figure 4.

[25] Figure 4a shows a peak for high-level clouds at 400 mb for ISCCP IR and above the 200 mb level for CloudSat-CALIPSO, while Figure 4b indicates that the largest peak for ISCCP VIS is at 500 mb, with a secondary maximum around 200 mb and a much smaller peak at 800 mb. There are considerably more clouds above 200 mb detected with CloudSat-CALIPSO than with ISCCP IR and VIS. To evaluate the contribution of optically thin clouds above the 200 mb level that probably only CALIPSO can detect (e.g., the clouds with a top near 15 km between 28° and 30°N in Figure 1), the CloudSat-only cloud top pressure estimate is also plotted in Figures 4a and 4b. The distribution based on CloudSat-only does not show a large peak above 200 mb, confirming the presence of high subvisible clouds, but instead two equivalent maxima, one at 200 mb and the other close to 300 mb. This demonstrates that some of the clouds above the 200 mb level detected with CloudSat-CALIPSO are in fact only detected with the lidar, and are thus optically very thin. It is quite probable that these clouds cannot be detected with passive remote sensing: *Haladay and Stephens* [2009] report a range of optical thicknesses between 0.02 and 0.3 for this type of cloud in the Tropics. However, CloudSat-only cloud top pressure at the peak is still lower than estimated with ISCCP IR and VIS. Thus these extremely thin clouds are not the only cause of the discrepancy.

[26] Overall, there is a larger bias in the ISCCP IR estimates at 192 ± 158 mb than the VIS estimates at 154 ± 195 mb, but with a lower uncertainty and higher correlation (see Table 2). When we separate day from night pixels, we find a slightly better agreement between ISCCP IR and CloudSat-CALIPSO cloud top pressures at night. In fact the nighttime bias in Table 2 is close to the bias obtained during the day with ISCCP VIS. With about the same number of IR pixels during both periods, the day-night IR difference cannot be attributed to sampling issues, thus we suspect that this has more to do with the cloud characteristics.

[27] *Liao et al.* [1995a] found a tendency for the ISCCP to miss the thinnest of the high-level clouds, which was confirmed in another assessment by *Jin et al.* [1996]. Also, according to *Liao et al.* [1995b] and later to *Stubenrauch et al.* [1999b], the largest errors in ISCCP cloud top pressures occur when there is more than one cloud layer in the atmospheric column or when the column optical thickness is low. Consequently here we investigate how the cloud optical thickness and the number of cloud layers can explain the differences between ISCCP and CloudSat-CALIPSO over the Tibetan Plateau.

[28] ISCCP provides coincident retrievals of column optical thickness. Figure 5a shows how the difference between ISCCP IR and VIS and CloudSat-CALIPSO cloud top pressure varies as a function of ISCCP optical thickness for August 2006. At an optical thickness of about 10, differences in cloud top pressure are confined within 150 mb for thicker clouds and increase up to 300 mb for thinner clouds. The correction applied for the ISCCP VIS cloud top pressure can be seen to improve the differences for optical thicknesses less than 5. This relationship is similar for

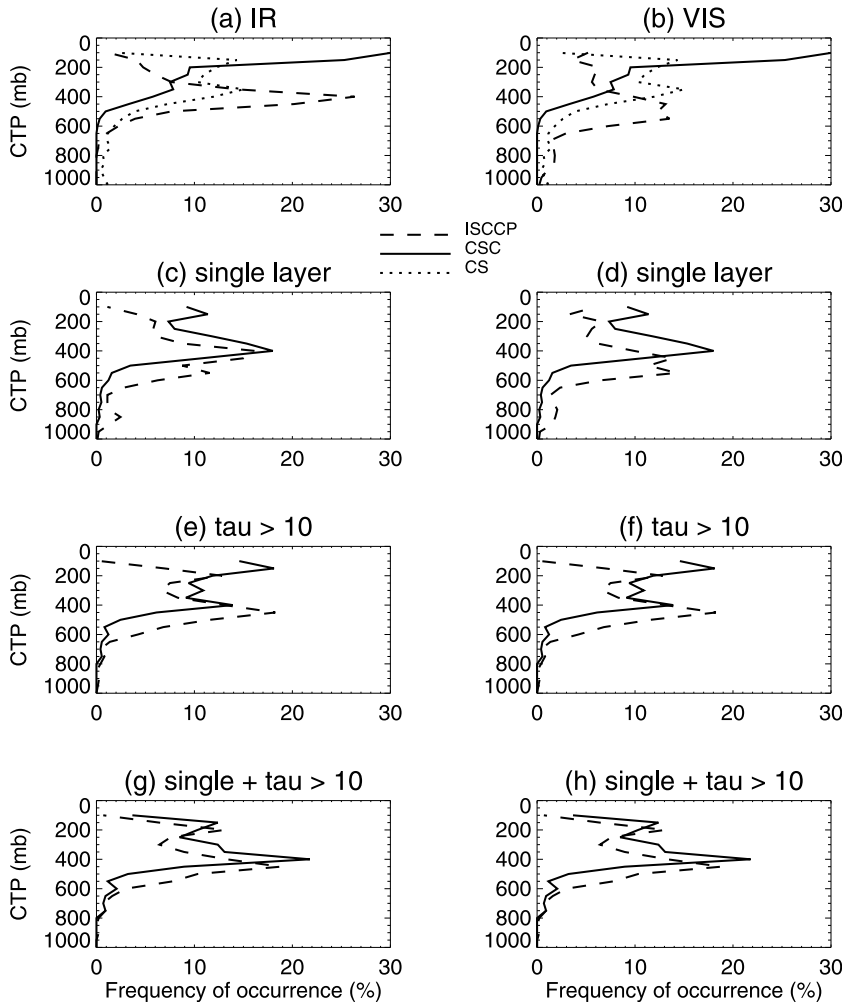

Figure 4. Cloud top pressure (CTP) frequency of occurrence for August 2006 over the Tibetan Plateau, when the ISCCP IR algorithm is used (left) and when the VIS algorithm is used (right), compared with CloudSat-CALIPSO (CSC) retrievals: (a, b) for all pixels, (c, d) for pixels where CSC detect a single cloud, (e, f) for pixels where the ISCCP optical thickness is greater than 10, and (g, h) for pixels where a single cloud with an optical thickness greater than 10 is present. The solid line represents CSC, the dashed line ISCCP IR or VIS, and the dotted line CloudSat only (CS).

February 2007 (Figure 5b), although the differences are smaller.

[29] CloudSat-CALIPSO profiles can reveal whether more than one cloud layer is present, and we use the median number of cloud layers for all profiles found in a DX-like portion to indicate if a DX pixel has more than one cloud layer. For the day-night difference in accuracy of the IR retrievals, we find that single-layer clouds occur more often during the day, so we suspect that the better agreement with CloudSat-CALIPSO at night comes instead from a larger

Table 2. Difference Between ISCCP IR and VIS and CloudSat-CALIPSO Cloud Top Pressures Measured Over the Tibetan Plateau in August 2006 for Different Subsets[a]

Subsets	IR-CSC CTP (mb) ± RMS	VIS-CSC CTP (mb) ± RMS
All cases	192 ± 158 R[b] = 0.43	154 ± 195 R = 0.33
Daytime	206 ± 186 R = 0.38	
Nighttime	178 ± 124 R = 0.35	
Single-level clouds	121 ± 134 R = 0.64 (50%)	83 ± 165 R = 0.53 (58%)
Multilayer clouds	263 ± 148 R = 0.28	251 ± 193 R = 0.15
Tau > 10 (daytime only)	109 ± 41 R = 0.49 (20%)	109 ± 141 R = 0.49 (42%)
Tau < 10 (daytime only)	276 ± 182 R = 0.35	186 ± 221 R = 0.24
1 layer, tau > 10 (daytime only)	52 ± 102 R = 0.72 (12%)	52 ± 102 R = 0.72 (25%)

[a]CSC, CloudSat-CALIPSO; CTP, Cloud Top Pressures.
[b]R equals correlation (% of pixels in subset).

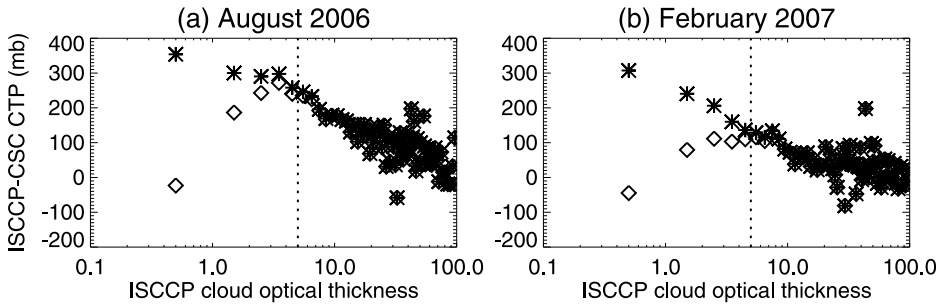

Figure 5. Difference between ISCCP and CloudSat-CALIPSO CTP for (a) August 2006 and (b) February 2007 over the Tibetan Plateau as a function of ISCCP derived cloud optical thickness when the IR algorithm is used (asterisks) and when the VIS algorithm is used (diamonds). The dotted line shows optical thickness equals 5.

occurrence of optically thick clouds at night. Unfortunately, we do not have optical thickness information at night to verify this.

[30] Table 2 and Figure 4 give the results of the comparison when pixels are retained that have (1) only a single-layer cloud (Figure 4c and 4d), (2) an optical thickness larger than 10 (Figures 4e and 4f) and (3) a single layer and an optical thickness larger than 10 (Figures 4g and 4h).

[31] 1. Figures 4c and 4d reveal that the two distributions become similar when only single-layer clouds are kept, although a small peak remains for low-level clouds in the ISCCP distribution not found in the CloudSat-CALIPSO distribution and an overall overestimate of cloud top pressures in the ISCCP can be noticed. The bias is about 120 mb for IR and 80 mb for VIS ISCCP cloud top pressures (Table 2).

[32] 2. Figures 4e and 4f show a bimodal distribution for high-level clouds with both data sets (ISCCP and CloudSat-CALIPSO) when thick clouds are considered ($\tau > 10$), with more high-level clouds found with CloudSat-CALIPSO and an overall bias of 110 mb for both IR and VIS ISCCP cloud top pressures.

[33] 3. The bias is significantly reduced when both restrictions are applied (Figures 4g and 4h), in particular for the highest of the clouds. Both data sets yield very similar distributions, with a slight bias for all clouds that appears to be larger in the 600–400 mb range. Thick single-layer clouds reveal a bias in ISCCP cloud top pressures of about 50 mb, an uncertainty of about 100 mb and a correlation with the CloudSat-CALIPSO estimates of 0.72.

[34] Some multilayer situations with an optically thick cloud above a low-level cloud will give fairly accurate ISCCP cloud top pressures. *Liao et al.* [1995b] found that ISCCP high-level cloud top pressures were close to limb viewing measurement estimates for about 20% of their observed multilayer cases. Here the difference in cloud top pressures between ISCCP VIS and CloudSat-CALIPSO was less than 100 mb for 22% of all multilayer cases in August 2006 with an average difference of -6 ± 109 mb.

[35] The remaining uncertainty is, in part, owing to the different nature of the measurements (e.g., passive versus active, IR/VIS versus mm/vis) and errors in collocation and coincidence. One possible measure of the error caused by the collocation is the standard deviation of the cloud top pressure per DX-like segment. This standard deviation represents the variability of the scene and characterizes the minimum possible difference between the two data sets. It is found to be 26 mb on average with a median value of 8 mb, both below the standard deviation of the difference. Thus the collocation problem is not explaining all of the remaining differences. Also, some uncertainties in the ISCCP temperature profiles may be responsible for some of the errors, as previously suggested by *Stubenrauch et al.* [1999a], but similarly there may be errors in the ECMWF geopotential height profiles that affect CloudSat-CALIPSO cloud top pressure estimates.

[36] We next investigate how the difference between the two retrievals varies with surface elevation. A previous comparison with an infrared sounder revealed a better performance of ISCCP over high topography for cloud detection [*Jin et al.*, 1996]. Figures 6a and 6b show the difference in cloud top pressure as a function of surface altitude for the ISCCP IR and VIS retrievals, respectively. For both techniques, the difference decreases as a function of altitude. In

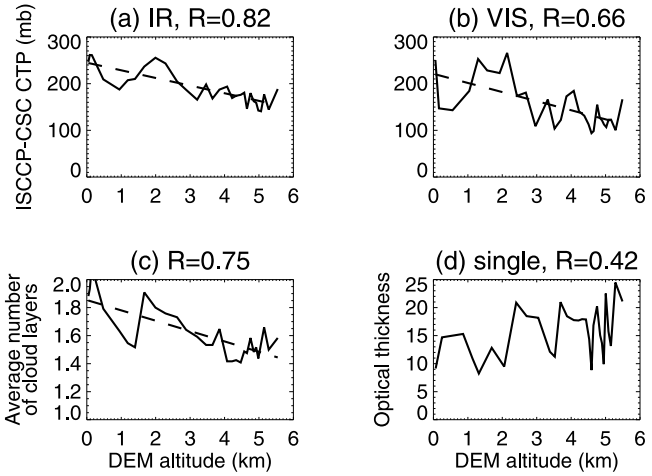

Figure 6. Relationship between the difference in CTP ISCCP-CloudSat-CALIPSO and the surface (digital elevation model) altitude averaged in 30 km pixels when using (a) the ISCCP IR retrieval and (b) the VIS algorithm; relationship between surface altitude and (c) the average number of cloud layers and (d) the optical thickness when one single layer is detected.

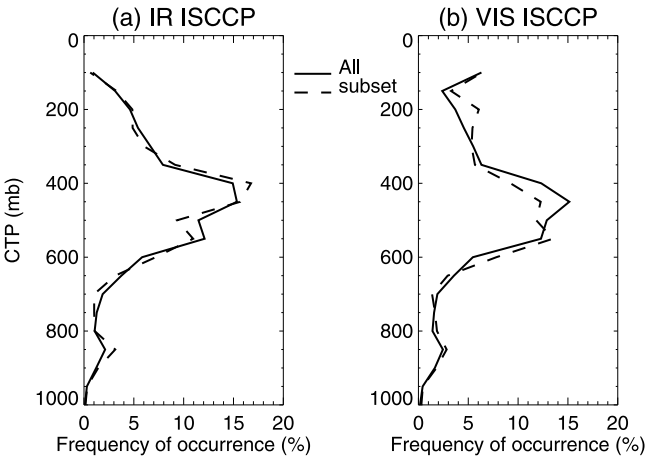

Figure 7. CTP frequency of occurrence using (a) IR and (b) VIS ISCCP retrievals for all DX pixels found in the Tibetan Plateau region in August 2006 (solid lines) and only those that have a CloudSat-CALIPSO orbit within 30 km and 90 min (dashed lines).

fact, Figure 6c shows that as altitude increases, the number of cloud layers decreases. Figure 6d reveals no clear correlation between column optical thickness and altitude. The difference in cloud top pressure did not show any correlation with variations (standard deviation) in surface altitude within a DX pixel either (not shown). We conclude that ISCCP IR and VIS cloud top pressures are more reliable at higher altitude primarily because multilayer clouds occur less frequently.

[37] Finally, we examine how CloudSat-CALIPSO sampling issues affect the cloud top pressure distributions by comparing ISCCP DX histograms obtained using all DX pixels within the Tibetan region in August 2006 with those that had a temporal and spatial match with the CloudSat-CALIPSO orbits. Figure 7 shows these histograms of cloud top pressures separately for the IR retrievals and the VIS retrievals. There are differences between the subset and the entire set of DX pixels, mainly between 400 and 600 mb for the IR cloud top pressure and also for high-level clouds for the VIS cloud top pressure (around 200 mb). However, it appears that in spite of the CloudSat-CALIPSO low sampling rate, it can still provide reasonable statistics at the monthly scale for this region.

3.3. Comparison for February 2007

[38] The same series of tests was performed using February 2007 observations. There are slightly more daytime detections (2733 out of 5060 pixels, 54%) for this month and more occurrences of clear sky pixels according to both data sets (see Table 3 for a summary of the cloud/clear pixel distribution according to both data sets). Similar results are found for the comparison between the two cloud masks; again clouds found close to the surface with CloudSat-CALIPSO are not always detected with ISCCP. The difference in cloud fraction is identical to August, but the variability larger, at 18 ± 15%.

[39] The agreement in cloud top pressure is much better though, probably because the occurrence of single-layer clouds dominates during this winter month (see Table 4). However, we also find more occurrences where ISCCP cloud top pressure is smaller than the CloudSat-CALIPSO estimate (note the VIS point at −45 mb in Figure 5b for $\tau \approx 0.5$). *Liao et al.* [1995b] had also noted this problem for high-level clouds in the mid-latitudes. Here the negative differences are found over pixels fully or partly filled with snow (~ 90–95% of all pixels with a negative difference in cloud top pressure between ISCCP and CloudSat-CALIPSO). The clouds are mostly single layer (80–90%) and optically thin (77% for VIS, 42% for IR have $\tau < 10$), and this is predominantly found with the VIS ISCCP cloud top pressure estimates rather than the IR estimates. This problem concerns 9% of the VIS and 4% of the IR cloud top pressures for February 2007, while this happened for only 3% of the VIS and 1% of the IR pixels in August 2006, also for optically thin single-layer clouds but without snow on the ground. Most of these clouds are found less than 5 km from the surface (80% of the clouds in summer, 48% in winter). The surface properties apparently affect the cloud signal in the visible, and this in turn affects the correction applied to the cloud top temperatures, making the clouds appear colder than they are. This makes the average bias much closer to zero for clouds with an optical thickness less than 10, a single layer, and within 5 km of the surface.

4. Implication for ISCCP D1 Accuracy Over the Tibetan Plateau

[40] To summarize, differences in cloud detection and cloud top allocation between ISCCP and CloudSat-CALIPSO are unrelated to the unusual topography and rugged terrain of the Tibetan Plateau. In fact, known problems with ISCCP (nighttime clouds close to the surface, multilayer clouds and low optical thickness) affect the accuracy of the ISCCP cloud detection and top pressures as much as they would anywhere else at these latitudes. Consequently, we now evaluate the frequency of occurrence of clouds within 5 km of the surface, of optically thin clouds, and of multilayer clouds at the seasonal scale to determine the overall accuracy of ISCCP D1 cloud retrievals over the Tibetan Plateau.

[41] Figure 8a shows the frequency of occurrence of single versus multilayer clouds by season. Multilayer clouds tend to occur more often in summer and less often in winter. Thus errors in cloud top pressure caused by multilayer clouds should be much reduced during winter.

[42] Figure 8b shows the frequency of occurrence of nighttime clouds below 5 km. Low-level clouds that may not be detected with the ISCCP algorithm tend to occur less often in summer and most often in the intermediate seasons. About 25% of the low-level clouds occur in winter and 22% in summer. The seasonal variations are small.

[43] Figure 9 shows the seasonal distribution of ISCCP cloud optical thicknesses over the Tibetan Plateau. The

Table 3. Same as Table 1 for February 2007

	CloudSat-CALIPSO DX-like Cloud Fraction		
ISCCP DX	0	1	0 < and < 1 (intermediate)
Clear	648	719	704
Cloudy	181	2335	473

Table 4. Same as Table 2 for February 2007

Subsets	IR-CSC CTP (mb) ± RMS	VIS-CSC CTP (mb) ± RMS
All cases	115 ± 147 R[a] = 0.52	59 ± 165 R = 0.52
Daytime	132 ± 162 R = 0.46	
Nighttime	84 ± 108 R = 0.64	
Single-level clouds	96 ± 139 R = 0.58 (80%)	46 ± 157 R = 0.56 (82%)
Multilayer clouds	190 ± 154 R = 0.41	113 ± 186 R = 0.34
Tau > 10 (daytime only)	30 ± 105 R = 0.72 (25%)	29 ± 105 R = 0.72 (39%)
Tau < 10 (daytime only)	199 ± 157 R = 0.46	78 ± 192 R = 0.45
1 layer, tau > 10 (daytime only)	21 ± 99 R = 0.76 (22%)	21 ± 99 R = 0.76 (35%)

[a]R equals correlation (% of pixels in subset).

thinnest of the clouds occur more often in winter and least often in summer, and on the contrary the intermediate to thick clouds occur more often in summer than in winter. Thus errors in ISCCP cloud top pressure caused by optically thin clouds should be reduced in the summer. However, larger optical thicknesses in the summer are related to the larger number of cloud layers then, since ISCCP optical thickness characterizes the total column. Thus, errors in cloud top pressures in the summer will be caused by a combination of multilayer and optically thin cloud layers. In the winter, cloud top pressure will be overestimated mostly because of optically thin clouds. Errors in optically thin cloud detection should be about the same for all seasons.

[44] Now that we have examined the seasonal variations in nighttime low-level clouds, in cloud optical thickness and multilayer occurrence, we investigate their impacts on ISCCP cloud top pressure seasonal distributions. Figure 10 shows the seasonal daytime cloud top pressure distributions for both data sets (ISCCP versus CloudSat-CALIPSO). Because the CloudSat radar is less sensitive to optically thin clouds than CALIPSO, we use the GEOPROF cloud mask alone to obtain the cloud top pressure of the highest layer in an attempt to eliminate high optically thin clouds from the cloud top pressure distribution ("CloudSat-only"). In addition, we select the CloudSat-CALIPSO cloud top pressure of the lowest cloud layer, to see if ISCCP is in better agreement with CloudSat-CALIPSO when the highest cloud in multilayer situations is ignored ("first layer").

[45] In summer, multilayer cloud situations occur more often than in other seasons, so we compare ISCCP with CloudSat alone to see if the large differences at low pressure levels are related to the presence of thin cirrus that are likely not detectable with passive sensors. Indeed, Figure 10b reveals that the distribution obtained with CloudSat alone is in much better agreement with ISCCP than CloudSat-CALIPSO. In addition, when the top of the lowest rather than highest cloud layer is used, the agreement is slightly better. In winter (Figure 10d), there are more single-level clouds, and this could explain the lower optical thicknesses than in other seasons. Thus low optical thickness clouds alone would explain the overestimate in ISCCP cloud top pressures. Indeed, when we compare ISCCP with the CloudSat-only or the top of the first layer cloud top pressure distribution, the agreement with ISCCP is slightly better but the improvement is not as large as in the summer. The slight underestimate of the winter low-level cloud occurrences in ISCCP could be caused by misdetections (Figure 8b). The fall distributions (Figure 10c) resemble the winter ones, but the improvement when using CloudSat-only or the first layer cloud top pressure is slightly greater than in winter. The spring distributions (Figure 10a) resemble the summer ones, although with less high-level clouds detected with CloudSat-CALIPSO and a smaller improvement when CloudSat-only or the first layer are used.

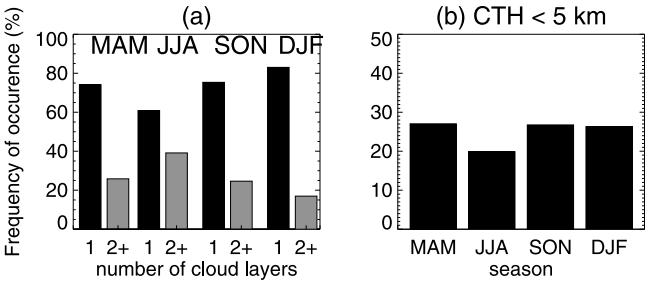

Figure 8. CloudSat-CALIPSO derived seasonal frequency of occurrence for one year over the Tibetan Plateau: (a) number of cloud layers normalized per season and (b) nighttime low-level clouds with a top height (CTH) within 5 km of the surface normalized to the total number of these clouds over a year.

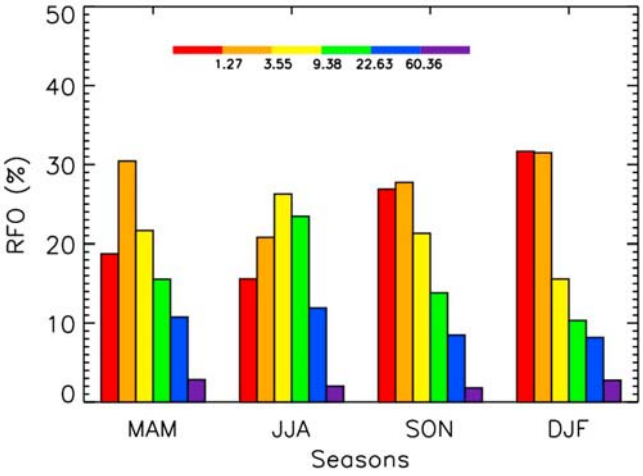

Figure 9. Relative Frequency of occurrence (RFO) of ISCCP cloud optical thickness distributed into the six intervals used in the ISCCP classification per season for 1 year over the Tibetan Plateau, normalized per season.

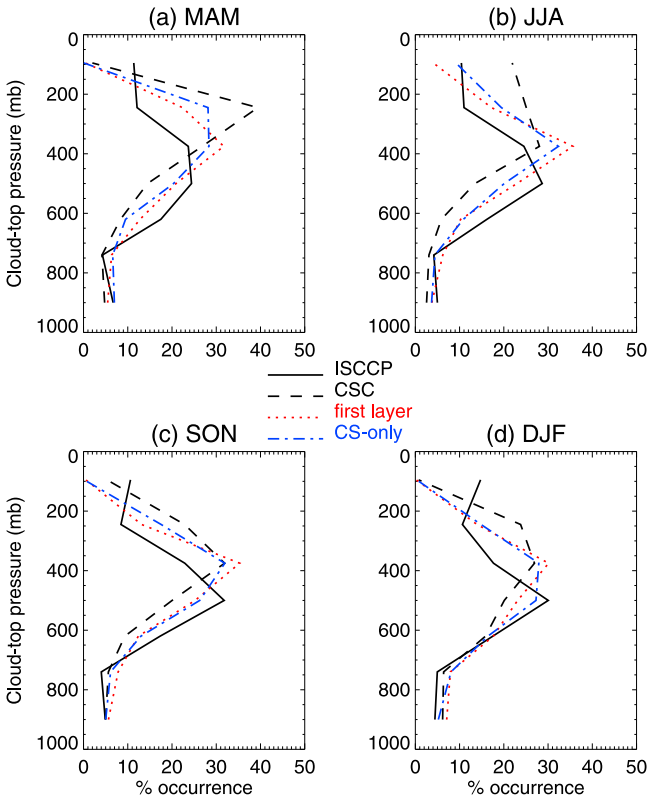

Figure 10. Seasonal CTP distribution from ISCCP (solid black line), CloudSat-CALIPSO (dashed black line), CS (blue dotted and dashed line), and using the lowest cloud layer (first layer) (red dotted line) over the Tibetan Plateau from July 2006 to June 2007.

[46] For all four seasons, the CloudSat-only and first layer cloud top pressure distributions are close to one another, suggesting that when more than one cloud layer occurs, the highest cloud layer is optically thin and often detected only by CALIPSO. Consequently, the remaining difference between ISCCP and CloudSat-only or the first layer cloud top distribution can be attributed mostly to the occurrence of optically thin clouds. This difference is fairly consistent from one season to another, suggesting that the distribution of optical thicknesses of the lowest or single layers is fairly similar from one season to another. In addition, the difference in cloud top pressure at the peak of the distribution for all seasons is about 100 mb, which is close to the accuracy in ISCCP cloud top pressure we found in the August 2006 and February 2007 comparisons (Tables 2 and 4).

[47] *Li et al.* [2006] conducted their comparison between ISCCP and ground observations using a high-middle-low cloud classification, so we also constructed histograms of the frequency of occurrence of each cloud type normalized to the total number of cloudy and clear sky observations (Figure 11). There are more high-level clouds detected with CloudSat-CALIPSO than ISCCP but the seasonal variations are similar, with a maximum in summer and a minimum in winter. Mid-level cloud occurrences are overestimated in ISCCP, and the seasonal variations are in opposite phase to CloudSat-CALIPSO, most likely because some seasons (e.g., winter) are not as affected by the multilayer cloud problem as others (e.g., summer). The frequency of occurrence of low-level clouds is small for both CloudSat-CALIPSO and ISCCP, and the seasonal variations appear out of phase. However, the frequencies are so small that it is difficult to evaluate if the phase difference is significant. When compared with Figure 2 of *Li et al.* [2006], the seasonal variations for ISCCP D2 are very similar for the three cloud levels to what we observe with D1, even if they use several years of observations instead of just the one here. If we compare the CloudSat-CALIPSO distribution with their weather station reports, it is clear that although the high-level clouds show similar seasonal variations, the midlevel and low-level clouds do not. This highlights how different ground-based reports of cloud level can be from the actual cloud level distributions.

5. Conclusions

[48] In this study we have investigated the accuracy of the 30 km 3 hourly ISCCP DX cloud detection and cloud top pressures in a high-elevation region: the Tibetan Plateau (25°N–40°N, 80°E–105°E). We compared these cloud top pressures with new and improved satellite estimates conjunctly obtained with two active instruments, CloudSat and CALIPSO. A method is proposed to reconcile the ISCCP sampling and measurement geometry with the vertical transects observed with the active instruments. Measurements from August 2006 and February 2007 over the

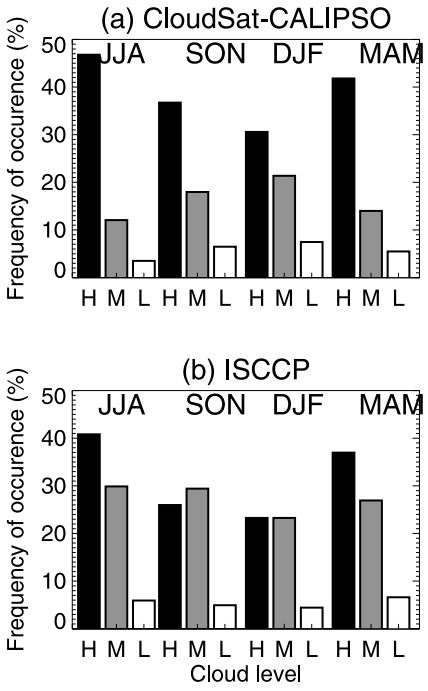

Figure 11. Seasonal distribution of high- (H), middle- (M), and low-level (L) clouds normalized to the total number of cloudy and clear observations for the entire Tibetan Plateau from July 2006 to June 2007, as observed with (a) CloudSat-CALIPSO and (b) ISCCP D1.

Tibetan Plateau revealed that the largest discrepancies between ISCCP and the active measurements occurred in multilayer cloud situations or when the cloud optical thickness was below 10 (consistent with *Liao et al.* [1995a, 1995b], *Jin et al.* [1996] and *Stubenrauch et al.* [1999b]) and are not directly correlated with surface elevation. We verify that CloudSat-CALIPSO low sampling rate in the region does not affect our conclusions.

[49] Consequently, we investigated the seasonal variations in multilayer cloud occurrence and cloud optical thickness distribution over the Tibetan Plateau. The occurrence of multilayer clouds is largest in summer when high-level optically thin clouds occur more often than in the other seasons. These clouds are very tenuous as only CALIPSO is able to detect them. The origin of these subvisible clouds in association with lower cloud layers in summer will be the subject of future research. Otherwise, when single-layer clouds are detected, the error in ISCCP cloud top pressure is of the order of 100 mb, and mainly caused by variations in cloud optical thickness. As far as detection capability is concerned, ISCCP experiences problems when low-level clouds are found within 4 km of the surface, and this is not correlated with the presence of snow on the ground, nor season-dependent. For all seasons, the highest elevations in the Tibetan Plateau seem to have less multilayer cloud occurrences, which will ensure much smaller biases than at lower elevations. This is encouraging for the use of the ISCCP climatology in high-elevation regions where surface stations are scarce.

[50] **Acknowledgments.** The CloudSat-CALIPSO GEOPROF-LIDAR and GEOPROF products were obtained from the CloudSat Data Processing Center, located at the Cooperative Institute for Research in the Atmosphere at Colorado State University in Fort Collins. The ISCCP DX and D1 products were obtained from the ISCCP research group at the NASA Goddard Institute for Space Studies, New York, New York. The authors would like to thank Violeta Golea for her help in retrieving the data and Yuan-Chong Zhang and James Miller for fruitful discussions. The authors thank three reviewers for their comments that improved this study.

References

Beniston, M. (2003), Climatic change in mountain regions: A review of possible impacts, *Clim. Change*, *59*, 5–31, doi:10.1023/A:1024458411589.

Beniston, M., H. Diaz, and R. Bradley (1997), Climatic change at high elevation sites: An overview, *Clim. Change*, *36*, 233–251, doi:10.1023/A:1005380714349.

Cui, X. F., and H.-F. Graf (2009), Recent land cover changes on the Tibetan Plateau: A review, *Clim. Change*, *94*, 47–61, doi:10.1007/s10584-009-9556-8.

Duan, A. M., and G. X. Wu (2006), Change of cloud amount and the climate warming on the Tibetan Plateau, *Geophys. Res. Lett.*, *33*, L22704, doi:10.1029/2006GL027946.

Haladay, T., and G. Stephens (2009), Characteristics of tropical thin cirrus clouds deduced from joint CloudSat and CALIPSO observations, *J. Geophys. Res.*, *114*, D00A25, doi:10.1029/2008JD010675.

Jin, Y., W. B. Rossow, and D. P. Wylie (1996), Comparison of the climatologies of high-level clouds from HIRS and ISCCP, *J. Clim.*, *9*, 2850–2879, doi:10.1175/1520-0442(1996)009<2850:COTCOH>2.0.CO;2.

Li, Z., W. X. Su, and Q. Z. Zeng (1998), Measurements of glacier variation in the Tibetan Plateau using Landsat data, *Remote Sens. Environ.*, *63*, 258–264, doi:10.1016/S0034-4257(97)00140-5.

Li, Y., X. Liu, and B. Chen (2006), Cloud type climatology over the Tibetan Plateau: A comparison of ISCCP and MODIS/TERRA measurements with surface observations, *Geophys. Res. Lett.*, *33*, L17716, doi:10.1029/2006GL026890.

Liao, X., W. B. Rossow, and D. Rind (1995a), Comparison between SAGE II and ISCCP high-level clouds 1. Global and zonal mean cloud amounts, *J. Geophys. Res.*, *100*, 1121–1135, doi:10.1029/94JD02429.

Liao, X., W. B. Rossow, and D. Rind (1995b), Comparison between SAGE II and ISCCP high-level clouds 2. Locating cloud tops, *J. Geophys. Res.*, *100*, 1137–1147, doi:10.1029/94JD02430.

Liu, X., and B. Chen (2000), Climatic warming in the Tibetan Plateau during recent decades, *Int. J. Climatol.*, *20*, 1729–1742, doi:10.1002/1097-0088(20001130)20:14<1729::AID-JOC556>3.0.CO;2-Y.

Liu, Y. H., J. R. Key, R. A. Frey, S. A. Ackerman, and W. P. Menzel (2004), Nighttime polar cloud detection with MODIS, *Remote Sens. Environ.*, *92*, 181–194, doi:10.1016/j.rse.2004.06.004.

Liu, Z., M. Vaughan, D. Winker, C. Kittaka, B. Getzewich, R. Kuehn, A. Omar, K. Powell, C. Trepte, and C. Hostetler (2009), The CALIPSO lidar cloud and aerosol discrimination: Version 2 algorithm and initial assessment of performance, *J. Atmos. Oceanic Technol.*, *26*, 1198–1213, doi:10.1175/2009JTECHA1229.1.

Mace, G. G., Q. Zhang, M. Vaughan, R. Marchand, G. L. Stephens, C. Trepte, and D. Winker (2009), A description of hydrometeor layer occurrence statistics derived from the first year of merged CloudSat and CALIPSO data, *J. Geophys. Res.*, *114*, D00A26, doi:10.1029/2007JD009755.

Marchand, R., G. G. Mace, T. Ackerman, and G. L. Stephens (2008), Hydrometeor detection using CloudSat-An Earth-orbiting 94-GHz cloud radar, *J. Atmos. Oceanic Technol.*, *25*, 519–533, doi:10.1175/2007JTECHA1006.1.

Niu, T., L. X. Chen, and Z. J. Zhou (2004), The characteristics of climate change over the Tibetan Plateau in the last 40 years and the detection of climatic jumps, *Adv. Atmos. Sci.*, *21*, 193–203, doi:10.1007/BF02915705.

Pu, Z., and L. Xu (2009), MODIS/Terra observed snow cover over the Tibet Plateau: Distribution, variation and possible connection with the East Asian Summer Monsoon (EASM), *Theor. Appl. Climatol.*, *97*, 265–278, doi:10.1007/s00704-008-0074-9.

Rangwala, I., J. R. Miller, and M. Xu (2009), Warming in the Tibetan Plateau: Possible influences of the changes in surface water vapor, *Geophys. Res. Lett.*, *36*, L06703, doi:10.1029/2009GL037245.

Rossow, W. B. (1993), Satellite orbit and data sampling requirements, in *Long-term Monitoring of Global Climate Forcings and Feedbacks*, NASA CP-3234, edited by J. Hansen, W. Rossow, and I. Fung, pp. 57–67, NASA, Washington, D. C.

Rossow, W. B., and L. C. Garder (1993), Cloud detection using satellite measurements of infrared and visible radiances for ISCCP, *J. Clim.*, *6*, 2341–2369, doi:10.1175/1520-0442(1993)006<2341:CDUSMO>2.0.CO;2.

Rossow, W. B., and R. A. Schiffer (1991), ISCCP cloud data products, *Bull. Am. Meteorol. Soc.*, *72*, 2-20, doi:10.1175/1520-0477(1991)072<0002:ICDP>2.0.CO;2.

Rossow, W. B., and R. A. Schiffer (1999), Advances in understanding clouds from ISCCP, *Bull. Am. Meteorol. Soc.*, *80*, 2261–2288, doi:10.1175/1520-0477(1999)080<2261:AIUCFI>2.0.CO;2.

Rossow, W. B., A. W. Walker, and L. C. Garder (1993), Comparison of ISCCP and other cloud amounts, *J. Clim.*, *6*, 2394–2418, doi:10.1175/1520-0442(1993)006<2394:COIAOC>2.0.CO;2.

Sèze, G., and W. B. Rossow (1991a), Time cumulated visible and infrared radiance histograms used as descriptors of surface and cloud variations, *Int. J. Remote Sens.*, *12*, 877–920, doi:10.1080/01431169108929702.

Sèze, G., and W. B. Rossow (1991b), Effects of satellite data resolution on measuring the space/time variations of surfaces and clouds, *Int. J. Remote Sens.*, *12*, 921952, doi:10.1080/01431169108929703.

Stephens, G. L., et al. (2002), The CloudSat Mission and the A-Train: A new dimension of space-based observations of clouds and precipitation, *Bull. Am. Meteorol. Soc.*, *83*, 1771–1790, doi:10.1175/BAMS-83-12-1771.

Stubenrauch, C. J., W. B. Rossow, F. Cheruy, A. Chedin, and N. A. Scott (1999a), Clouds as seen by satellite sounders (3I) and imagers (ISCCP). Part I: Evaluation of cloud parameters, *J. Clim.*, *12*, 2189–2213, doi:10.1175/1520-0442(1999)012<2189:CASBSS>2.0.CO;2.

Stubenrauch, C. J., W. B. Rossow, N. A. Scott, and A. Chedin (1999b), Clouds as seen by satellite sounders (3I) and imagers (ISCCP). Part III: Spatial heterogeneity and radiative effects, *J. Clim.*, *12*, 3419–3442, doi:10.1175/1520-0442(1999)012<3419:CASBSS>2.0.CO;2.

Tegen, I., and I. Fung (1994), Modeling of mineral dust in the atmosphere: Sources, transport, and optical thickness, *J. Geophys. Res.*, *99*, 22,897–22,914, doi:10.1029/94JD01928.

Wang, B., Q. Bao, B. Hoskins, G. X. Wu, and Y. M. Liu (2008), Tibetan Plateau warming and precipitation changes in East Asia, *Geophys. Res. Lett.*, *35*, L14702, doi:10.1029/2008GL034330.

Winker, D. M., et al. (2009), Overview of the CALIPSO mission and CALIOP data processing algorithms, *J. Atmos. Oceanic Technol.*, *26*, 2310–2323.

Wu, Q. B., and T. J. Zhang (2008), Recent permafrost warming on the Qinghai-Tibetan Plateau, *J. Geophys. Res.*, *113*, D13108, doi:10.1029/2007JD009539.

Yao, T. D., Y. Q. Wang, S. Y. Liu, J. C. Pu, Y. P. Shen, and A. X. Lu (2004), Recent glacial retreat in High Asia in China and its impact on water resource in northwest China, *Sci. China, Ser. D: Earth Sci.*, *47*(12), 1065–1075.

You, Q. L., S. C. Kang, E. Aguilar, and Y. P. Yan (2008), Changes in daily climate extremes in the eastern and central Tibetan Plateau during 1961–2005, *J. Geophys. Res.*, *113*, D07101, doi:10.1029/2007JD009389.

Y.-H. Chen and C. M. Naud, Department of Applied Physics and Applied Mathematics and NASA Goddard Institute for Space Studies, Columbia University, 2880 Broadway, New York, NY 10025, USA. (cnaud@giss.nasa.gov)